Construction of the Environment Map on the Basis of Local Alignment

R. Mahkovic B. Petelinkar
Faculty of Computer and Information Science
University of Ljubljana
1000 Ljubljana, Slovenia
e-mail: *rajko.mahkovic@fri.uni-lj.si*

Abstract — The local alignment method of scan data frames obtained by some scanning device, such as laser range scanner, needed in global map building, is presented. The method does not require some specific environment. It is based on the alignment of two consecutive scan data frames, obtained in the exploration of the static environment. The exploration is realized by the use of the local Voronoi diagrams of the visible region. The position of the next scanning action is determined from this local Voronoi diagram. All the points from the compared scan data frame are tried to be fitted to all the segments of the base scan data frame. The intervals - the translational displacement and the rotation - on which the majority of the points correspond to the segments are incrementally narrowed. This leads to a more correct position of a data frame in the global map.

1 Introduction

We address the problem of building a map of the unknown environment from sensor data supplied by some range scanning device such as sonar or laser range scanner. We call the collection of range measurements in a plane, taken at some position, a *scan data frame*. Scan data frame is associated with the position and the orientation of the robot at the moment of the measurement. Since we assume that only *relative* measurement of the position is available, the values of the position and orientation associated with scan data frames are uncertain, due to the accumulating nature of relative position measurement. In a local scan data frame, the relative object positions with respect to the robot position and orientation are fixed. Their uncertainty is determined by the bounded errors of the sensor.

Range scans were used in previous robotic systems for robot self localization in known environments, Cox [1], or for modeling an unknown environments, Crowley [2], Leonard and Durrant-Whyte [4] and Gonzales et al. [3].

A generally employed approach of building a global map is to incrementally integrate new data frames into a global map. The current data frame is aligned to the previous data frames or to a global model after the measurement. Our approach is different from those methods in which the integration of the new data frame is based on the *recognition* of the objects. Instead, we align the current data frame with the previous one solely on the basis of the measured points in them (similar to the approach of Lu and Milios [5]). By the *alignment* we mean just the readjustment of relative differences in their positions and orientations, as supplied by the odometric system. Since we keep all the data frames in memory, the alignment is possible also later in the further process of exploration.

2 Environment exploration

A robot is placed at the beginning somewhere in the working space which is completely unknown to it; the position as well as the shape of the obstacles are not known. Its task is to acquire the map of the environment; however, the robot is not expected to build the *representation* of the environment in the sense of some, for example, geometrical forms - it is required only to integrate the local scan data frames into a global map.

2.1 GLVD from local scan

The robot starts with the scanning action from the start position. The position of this first local observation of the environment served him as the coordinate origin of the map. All of the subsequent scan data frames are incrementally integrated into the global map; the rough displacement between two scanning positions is given by the odometric system, which is the basis for much finer matching of the frames by the procedure of local alignment.

The exploration is realized by the use of the *generalized local Voronoi diagram*, GLVD [6, 7], which is constructed on the basis of scan points in a frame. Although the robot is not obliged to follow the diagram exactly, this remains quite desirable, since the Voronoi diagram offers the robot the possibility to keep up the maximal free distance to the nearest obstacles - this property is the major advantage of the diagram. Also, the local Voronoi diagram offers the robot the possibility to accomplish only really 'necessary' number of scanning actions, since the *marginal points* of its validity may be determined [7], which are the points where the match between the local Voronoi diagram and the global Voronoi diagram of the environment ends. These are precisely the points where another scan action is needed, due to the limited visibility from the previous scanning position. The robot explores the

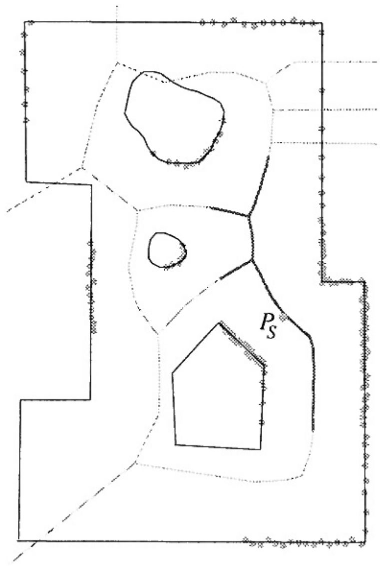

Figure 1: GLVD constructed at P_S.

environment by actually following the edges of the global Voronoi diagrams. The exploration is in fact an implementation of the depth search of a graph - generalized Voronoi diagram - whose nodes are Voronoi points, the points where at least three edges join together. (In this paper we shall neglect the problem of exploration of dead-end regions, which would lead to a modification of the exploration. We assume that convex regions are observable at least at one point on the global Voronoi diagram.) One GLVD constructed from a local scan obtained from P_S may be observed in Fig. 1: bold line segments denote a *regular* part of the GLVD that corresponds to a particular part of the global diagram of the environment, while the light line segments differ from it substantially, due to the limited visibility from P_S. We may observe the global Voronoi diagram of the same environment in Fig. 5. The diagram is situated in the middle of the free space between the obstacles and the boundary and consists of four Voronoi points - nodes - connected by six edges. The four marginal points of the GLVD from Fig. 1 are the points between the bold and the light segments. Each one denotes the position where the next scanning operation in a particular Voronoi edge is needed.

3 Local alignment

The local alignment consists of matching two frame scans, obtained by two, either spatially or timely, adjacent observations of the local environment. By *matching* we mean that the next scan frame, *compared scan frame*, is tried to be as much as possible aligned with the previous one, which in turn is aligned with the one 'before it', and so on. That is, all the scan frames are not aligned with respect to some *global* point - origin point -, instead, they are aligned *relatively* to each other where the first scan frame, *base scan frame* represents the 'origin'. We denote the set of all segments, obtained by connecting the successive scan points of the base scan frame, by *base segment set* - BSS , whereas the set of all points in compared scan frame by *compared point set* - CPS (in fact, there are not really *all* the segments which are included in BSS; the segments between two clusters, i.e., the segments connecting the scan points from two different objects - see [7] - are excluded since they do not represent the objects).

3.1 Point on segment

The process of alignment of the compared scan frame with the base scan frame is realized through the alignment of each point in CPS with each segment in BSS. The alignment process is demonstrated in Fig. 2: a point $p_i = (x, y)$ from CPS is rotated with respect to O so as to determine the interval of feasible rotations. Regarding only its x component, point p_i could originate from the segment s_j if the value of its rotation was from the interval F_x; note that the interval of x component of the segment is expanded by the maximal estimated odometric error (accumulated from the base frame to comparing frame) Δx. Analogous holds for the y and φ component. F_x, F_y and F_{x+y} are therefore the intervals of feasible rotations of p_i, such that x, y and their sum agree with the components of the segment. F_i then denotes the whole feasible rotation determined by $F_i = F_\varphi \cap F_x \cap F_y \cap F_{x+y}$, where $F_\varphi = [-\Delta\varphi, \Delta\varphi]$.
Let (x', y') denote the *correct* position of the point p_i. This point can be related, due to the translational and the rotational errors dx, dy, $d\varphi$, the mobile robots produces when moving from one scanning position to the next, to the measured point by the equation

$$\begin{bmatrix} x' \\ y' \end{bmatrix} = \boldsymbol{R}_\varphi \begin{bmatrix} x \\ y \end{bmatrix} + \begin{bmatrix} dx \\ dy \end{bmatrix}. \qquad (1)$$

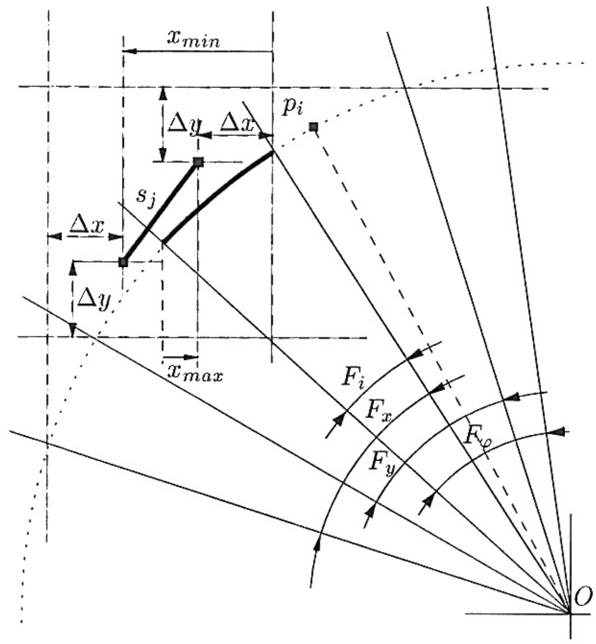

Figure 2: The alignment of point with the segment: a scan point is rotated with respect to scanning location of the previous scan frame to determine the rotating interval of the best alignment with a given segment.

In the equation, the quantity $\boldsymbol{R}_\varphi$ represents the rotational matrix

$$\boldsymbol{R}_\varphi = \begin{bmatrix} \cos\varphi & -\sin\varphi \\ \sin\varphi & \cos\varphi \end{bmatrix}.$$

The translational errors are supposed to lie in the experimentally determined intervals: $dx \in [-\Delta x, \Delta x]$ and $dy \in [-\Delta y, \Delta y]$; if the movements of the robot are measured by an odometric system, these intervals can be determined quite reliably. We may assume then that the correct point lies in the following interval

$$x' \in [min(x_1, x_2) - \Delta x, max(x_1, x_2) + \Delta x] \quad (2)$$

$$y' \in [min(y_1, y_2) - \Delta y, max(y_1, y_2) + \Delta y]. \quad (3)$$

Taking into account the rotation only, we may write the inequations

$$min(x_1, x_2) - \Delta x \leq x\cos\varphi - y\sin\varphi \leq max(x_1, x_2) + \Delta x$$
$$min(y_1, y_2) - \Delta y \leq x\sin\varphi + y\cos\varphi \leq max(y_1, y_2) + \Delta y.$$

We may determine then the intervals of feasible rotations by using the equation

$$a\sin\varphi + b\cos\varphi = \operatorname{sgn}(a)\sqrt{a^2+b^2}\sin(\arctan(b/a) + \varphi). \quad (4)$$

This is how the rotation intervals F_x, F_y, F_{x+y} and consequently F_i, mentioned above, are calculated. Given the feasible rotation interval F_i, the intervals X_i and Y_i of feasible translations along both axis can be determined. Only the boundary values x_{min} and x_{max} for X_i are indicated in Fig. 2 ($X_i = [x_{min}, x_{max}]$).

The solution of point-to-segment alignment is characterized by the triplet (F_i, X_i, Y_i).

3.2 The alignment of two data frames

In the algorithm we try to achieve alignment of the points from the compared data frame with the segments from the base data frame. Its core is the alignment of a point on a segment, described above. The whole procedure is based on '*voting*'. The translational displacement is expected to be from some interval - for x component, for example, this is the interval $[-\Delta x, \Delta x]$. This interval is uniformly distributed into, say, 50 subintervals. For each of the subintervals the associated counter is maintained which represents one entry in the array of counters covering the whole interval, CAx. Similarly, the interval $[-\Delta y, \Delta y]$ is 'covered' by CAy array and the interval with rotation values $[-\Delta\varphi, \Delta\varphi]$ by CAφ. Each time a point can be fitted into a segment, using the translational and rotational values which fall into the intervals, the appropriate counters are incremented, depending on which subintervals the current values fall in.

In addition to separate arrays of counters, a composite array of counters CAxyφ exists which counts the occurrences when a displacement suits to all three intervals simultaneously.

At last, we maintain also a *boolean* variant of all the arrays, CAx$_i$, CAy$_i$, CAφ_i, CAxyφ_i; they are set/reset according to the result of a single point-to-segment alignment.

The essential part of an alignment of two data frames is given by the following procedure.

Procedure AllPntsToAllSegs:
Initialize arrays CAx$_i$, CAy$_i$, CAφ_i, CAxyφ_i to 0
For $\forall\ p_i \in$ CPS
begin
For $\forall\ s_j \in$ BSS
begin
Compute the relevant triplets (F_i, X_i, Y_i)
(for current p_i and s_j);
Set/reset the appropriate
CAx$_i$, CAy$_i$, CAφ_i, CAxyφ_i
according to subintervals with the solutions;
end
CAx = CAx + CAx$_i$;
CAy = CAy + CAy$_i$;
CAφ = CAφ + CAφ_i;
CAxyφ = CAxyφ + CAxyφ_i;
end

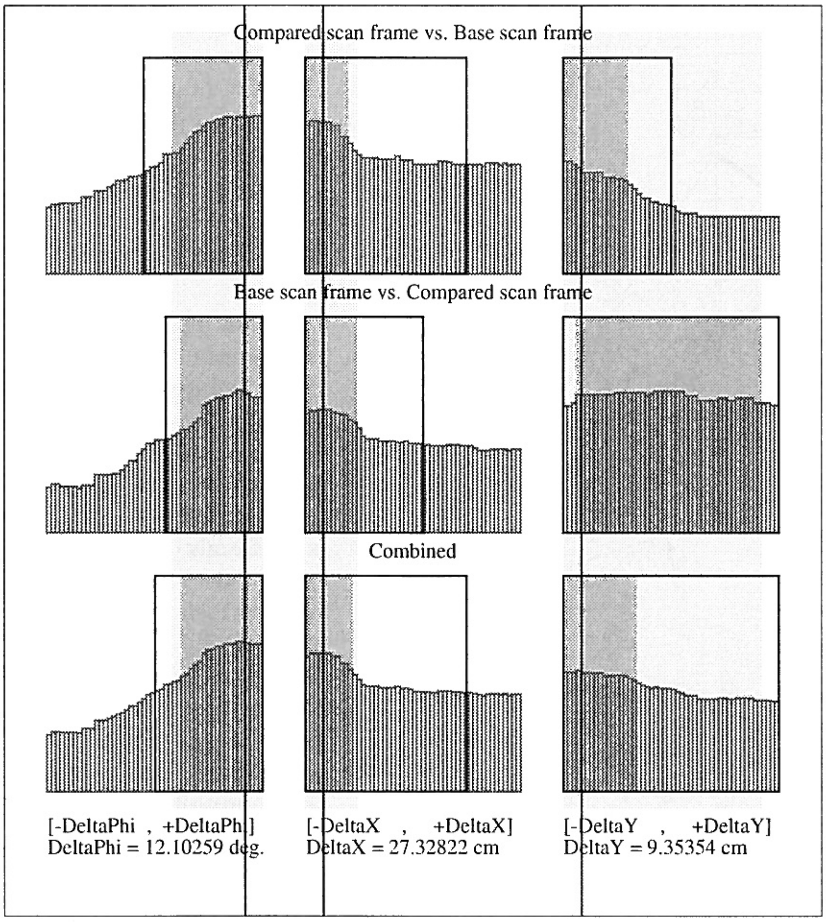

Figure 3: Illustration of voting.

The output of the procedure are the arrays CAx, CAy, CAφ and CAxyφ in which the maximal values can be found. We are interested actually in the corresponding subintervals. The new values for Δx, Δy and $\Delta\varphi$ are determined by centering the new - narrower - intervals around these maximal values by leaving only the subintervals in which a prescribed number of points fall (the number is determine experimentally). The procedure is repeated as long as the intervals are being narrowed. Fig. 3 illustrates one loop of the narrowing procedure. The three columns of pictures represent three intervals $[-\Delta\varphi, \Delta\varphi]$, $[-\Delta x, \Delta x]$, and $[-\Delta y, \Delta y]$. The three rows are the histograms representing the voting results over the intervals. The first row resulted from the alignment of all the points from the compared scan frame to all the segments from the base scan frame, the second from the reversed situation, and the third from their combination. Light and heavily shaded rectangular regions indicate, with respect to XY- or XYR-space, the new intervals. Additionally, three vertical lines representing the *correct* values are drawn.

The process of local alignment is normally applied to consecutive scan data frames. However, when the Voronoi point on the diagram is reached, the data frame acquired at that point can be aligned with all the nearest scan data frames from all the edges originating in the Voronoi point. Note that this implies the *recognition* of the previously discovered Voronoi points (represented in the robot in terms of position and orientation of the emanating edges) of the environment. Since this recognition is only possible within some tolerances, there must not be another Voronoi point within a prescribed distance.

4 Experimental results

In this section we give some simulational results in which laser scanner with no angular error and $\pm 4cm$ distance error was modeled. The tested environment had three obstacles in it. The shape of the obstacles and the shape of the environment was not prescribed. In Fig. 4 all the local scan data frames are shown in the coordinate system of the base data frame. The scan points of the subsequent 24 data frames - it took 25 scanning actions to explore the whole environment - are distributed widely along the borders of the objects, which is due to a relatively large (10%) odometric error.

Fig. 5 shows the same 25 scan points *after* the local alignment of all frames. More aligned scan frames resulted also in smoother generalized Voronoi diagram of the environment.

The exploration order as well as the difference between the correct and the actual scanning position may be seen in Fig. 6. To compare the results of the local alignment,

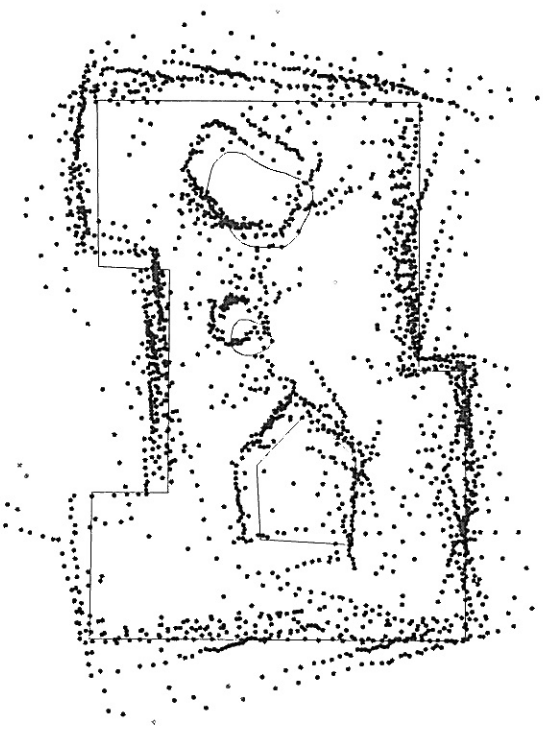

Figure 4: The local scan data frames placed into the global map according to the displacement determined by odometric system only.

we implemented the global alignment method, described by Lu and Milios [5]. The results of the comparison may be observed on three pictures in Fig. 7 in which the errors (ordinate axis) versus scan data frames (abscissa) are plotted. We may observe, from top to the bottom, the translational errors in x and y component, as well as the error in the orientation for unaligned frames (dotted line), for locally aligned frames (solid) and for globally aligned frames (dashed). Local alignment reduced the errors substantially, while the final global alignment is normally still beneficial.

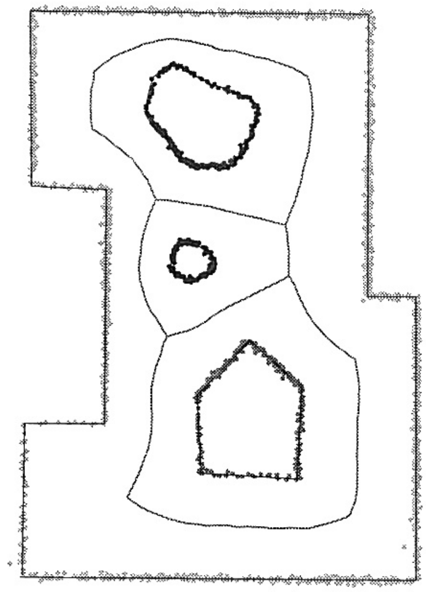

Figure 5: The local scan data frames after the local alignment.

5 Conclusions

We presented a novel local alignment procedure which aligns the compared scan data frame with the base scan data frame. The scan data frames may be obtained by some scanning device, such as laser range scanner. The procedure attempts to align all the points of the compared data frame to all the segments of the base frame. The translational and the rotational intervals which correspond to the most of the compared points are subsequently narrowed. The environment is explored with the use of the local Voronoi diagrams of the visible region, which represent the valid parts of the global Voronoi diagram of the environment and which determine the position of the next scanning. The alignment is made between two frames acquired at the nearest scanning positions and between all the frames around Voronoi points in the global Voronoi diagram. The results of the local alignment were compared with the results of further global alignment method of Lu and Milios [5]. It was demonstrated that the local alignment reduced the translational and rotational errors considerably.

The application of the alignment method is not limited to the environments with the specific type of obstacles.

References

[1] I.J. Cox. Blanche: An experiment in guidance and navigation of an autonomous robot vehicle. *IEEE*

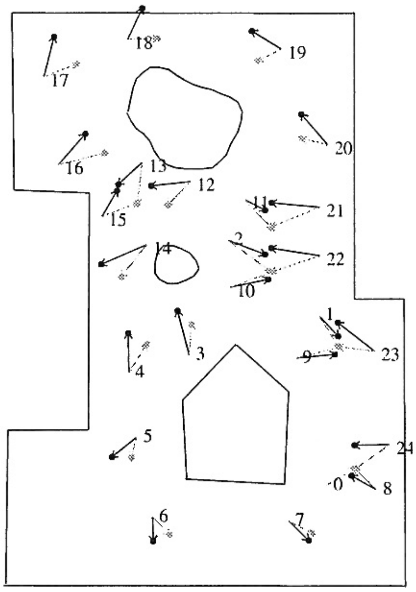

Figure 6: Correct (light grey points) and actual (dark grey points) scanning positions during the exploration. Thee scanning actions are numbered.

Transactions on Robotics and Automation, 7(2): 193 - 204, 1991.

[2] J.L. Crowley. World modeling and position estimation for a mobile robot using ultrasonic ranging. In *IEEE Int. Conf. on Robotics and Automation*, pages 674 - 680, 1989.

[3] J. Gonzales, A. Reina, and A. Ollero. Map building for a mobile robot equipped with a 2D laser rangefinder. In *IEEE Int. Conf. on Robotics and Automation*, pages 1904 - 1909, 1994.

[4] J.J. Leonard and H.F. Durrant-Whyte. *Directed Sonar Sensing for Mobile Robot Navigation.* Kluwer Academic Publishers, Boston, 1992.

[5] F. Lu and E. Milios. Globally Consistent Range Scan Alignment for Environment Mapping. *Autonomous Robots*, 1(4): 333 - 349, 1997.

[6] R. Mahkovic. Construction of the Generalized Voronoi diagram of the unknown environment. In *Proc. IEEE Int. Symposium on Industrial Electronics*, pages 984–989, Bled, Slovenia, 1999.

[7] R. Mahkovic and T. Slivnik. Constructing the Generalized Local Voronoi Diagram from Laser Range Scanner Data. *IEEE Transactions on Systems, Man, and Cybernetics, Part A*, 30(6): 710–719, 2000.

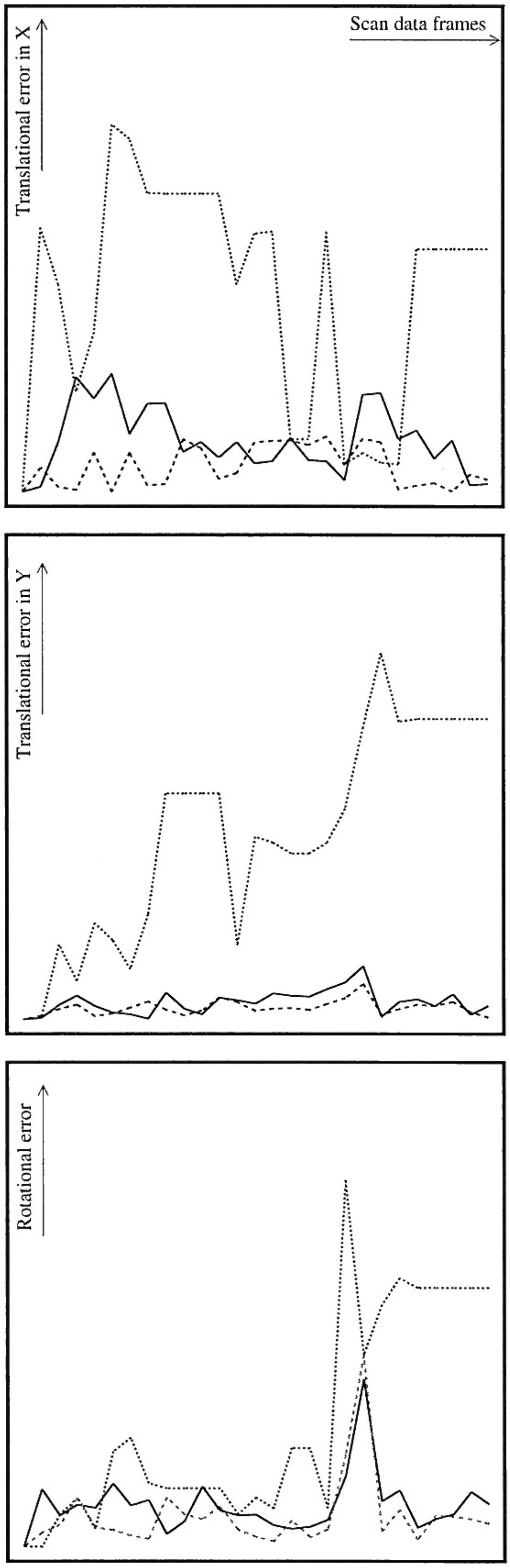

Figure 7: Translational and rotational errors with respect to scan data frames: original errors (dotted), errors after the local alignment (solid), and the errors after three loops of global alignment (dashed).